Available online at www.elixirpublishers.com (Elixir International Journal)

Applied Chemistry

Elixir Appl. Chem. 92 (2016) 38764-38773

ISSN: 2229-712X

Effect of Biocide on the Stability of Pomegranate Peel and Roselle as Eco-friendly Inhibitor on the Corrosion Control of Mild Steel in Acidic Medium

M.M.B.El-Sabbah[1*], A.Z. Gomaa[2], M.H.Mahross[3], H.F.Y.Khalil[1] and B.N.A.Mahran[4]

[1]Chemistry Department, Faculty of Science, Al-Azhar University, Nasr City, Cairo, Egypt.

[2]Paint Consultant

[3]Chemistry Department Faculty of Science, Al-Azhar University, Assiut, Egypt

[4]Laboratory for Environment Quality Monitoring, National Water Research Center, Egypt

ARTICLE INFO

Article history:

Received: 16 January 2016;

Received in revised form:

1 March 2016;

Accepted: 4 March 2016;

Keywords

Aqueous extract of pomegranate peel and roselle,

Mild steel,

Inhibitors,

Surface morphology.

ABSTRACT

The aqueous extract of Pomegranate Peel and Roselle (AE Pom P and Ros) has been studied as a possible source of green inhibitor for the corrosion of mild steel in 1 M HCl at temperature range 25-55^{o} C utilizing the conventional weight loss, open circuit potential (OCP) , linear and Tafel polarization techniques. The assessment of (AE Pom P and Ros) against different microorganisms has additionally been providing by using selected biocide. Moreover the structure of (AE Pom P and Ros) is analyzed by GC-MS spectra. The optimum dose of biocide which showed good stability for the corrosion inhibitor for more than one year , diminishes the inhibition efficiency for about 20% due to its slightly acidic in nature (pH=4).The inhibition efficiency was found to increase with increasing concentration of the inhibitor and with decreasing temperature. The adsorption of (AE Pom P and Ros) on the mild steel surface obeys the Langmuir adsorption isotherm. Polarization studies indicate that the (AE Pom P and Ros) is mixed type inhibitor. The thermodynamic functions of adsorption processes were calculated from weight loss at different temperatures data and were used to analyses the inhibitor mechanism. The surface morphology of the mild steel specimens was evaluated using SEM and EDAX analysis.

Introduction:

Mild steel is one of the most widely utilized engineering materials, despite its relatively limited corrosion resistance. Corrosion is one of the main concerns in the durability of metallic materials and their structures. Numerous endeavors have been made to develop a corrosion inhibition process to prolong the life of existing structures and minimize corrosion damages [1].

The strict environmental legislations and increasing ecological awareness among scientists have led to the development of "green" alternatives to mitigate corrosion [2]. The corrosion control of metals is of technical, economical, environmental, and aesthetical importance. The use of inhibitors is one of the best options of protecting metals and alloys against corrosion. The environmental toxicity of organic corrosion inhibitors has prompted the search for green corrosion inhibitors as they are biodegradable, do not contain heavy metals or other toxic compounds. In addition to being environmentally friendly and ecologically acceptable, plant products are inexpensive, readily available and renewable [3].

Dried petal of Roselle is mainly used for food, beverages (tea) as well as food coloring agent, as it has been known that it contains anthocyanins, delvinidin-3-monoglucosyde and cyanidin-3-monoglucoside [4-6]. Anthocyanins are generally found in red, purple and blue flowers. Anthocyanins tend to have no color in solution with neutral pH value, intense red in very acidic solution and blue in basic solution [7, 8].

Pomegranate (*Punicagranatum* L.) has been described as a rich source of (poly) phenolic components, with a broad array of different structures (phenolic acids, flavonoids, and hydrolyzable tannins) [9].

Punica granatum is from the family Punicacea. It grows in all warm countries of the world and was originally a native of Persia [10]. The rind of pomegranate contains a considerable amount of tannin, about 19% with pelletierine [11, 12].

The objective of this study to investigate the effect of pomegranate peel and Roselle extract as green corrosion inhibitor for the mild steel in 1.0 M HCl at different temperatures by using weight loss, OCP, linear and Tafel polarization techniques. The effects of temperature were also studied. The evaluation (AE Pom P and Ros) against different microorganisms has also been providing by using biocide.

Experimental:

Materials:

The mild steel specimens tested in the present study are in the form of sheet, the designation and analysis of the material is given in Table (1).

Before immersion the obvious electrode in the test solution each of them is prepared by polishing with emery paper from 250 to 1200 grade to obtain a smooth surface, washing with distilled water and then degreased with acetone about 5 minutes, washed again with distilled water then dried using filter papers.

Tele:

E-mail address: mmbel_sabbah@hotmail.com

Table 1: Chemical Composition of Mild Steel by Wt %

C	Si	Mn	P	S	Cr	Mo	Fe
0.06495	0.02057	0.11096	0.00446	0.00348	0.0000	0.00167	99.7703
Co	**Cu**	**Ti**	**V**	**W**	**Ni**	**Al**	
0.00399	0.02099	0.00110	0.00000	0.00000	0.00430	0.02513	

Preparation and extraction of the plant extract:

Pomegranate Peel Extraction:

Preparation of Raw Material: The samples were collected and washed thoroughly with water to remove any impurities. After drying at room temperature, the samples were ground into powder with the help of grinder.

Extraction of Crude Dyestuff: 100 g of sample was weighed and taken in a round bottom flask and 500ml of solvent (ethanol / water) in the ratio 40:60 was added to it. The flask was heated in a water bath at 60°C for 60mins.The solution was then filtered to obtain crude dyestuff.

Purification of Crude Dyestuff: The crude dyestuff is distilled to get 1/3rd of the solution using the Soxhlet apparatus at 70°C for 3hrs. In this process ethanol is recovered and the concentrated dye is obtained. The solution is kept overnight at room temperature for precipitation. The precipitation in ethanol / water is obtained by decanting the solution. The obtained particles are dried in the oven overnight at 60°C. Water was added in the Soxhlet apparatus. By addition of water, the boiling points of the compounds are lowered, allowing them to evaporate at lower temperatures [13].

Roselle Extraction:

Each plant materials (kenaf [Hibiscus cannabinus L.] seeds, roselle (Hibiscus sabdariffa L.) seeds and roselle calyxes) were grounded into fined powder using grinder to reduce the particles size respectively. The dried sample powders (500 g) were placed in a 2000 mL round-bottom flask with 1300 mL of deionised water, respectively in order to carry out hydro distillation for 4 hours or until there was no more essential oil yield. After 4 hours, the liquid retentate from each hydrodistillation were centrifuged at 4500 rpm for 20 minutes and the supernatant was filtered using filter paper to obtain a clear solution of water extract. The collected filtrates were then undergone rotary evaporation at 45°C using rotary evaporator until sticky extracts were obtained. The sticky extracts obtained were oven dried at 65°C for 1 day to remove excessive water. It was then kept at -20°C prior to further use. [14]

Gas Chromatography / Mass Spectrometry (GC/MS):

The analyses of (AE Pom P and Ros) were performed on an Agilent 7890A GC/5975C MSD system. Mass-Hunter WorkStation software was used for structure verification.

Evaluation of the effect of biocides (BIOPOL-TC/3) on (AE Pom P and Ros):

Detection and isolation of different microorganisms:

The pure cultures of different bacteria isolated were identified by conventional bacteriological test methods and by reference to the keys outlined for Bacillus subtilis by (Baklola, 2013)[15], Pseudomonas aeruginosa by(APHA, 2005) [16], Escherichia coli by (Pettibone, 1992) [17], pseudomonas fluorescens (Cappuccino and Sherman, 2002) [18] and Staphylococcus aureus by (APHA, 2005) [16].

Purification and identification of bacterial isolates:

Bacterial colonies developed from all previously mentioned media were chosen and picked up according to variation in culture characteristics and colony formation then purified by streak-plate method on nutrient agar medium (Difco) of the following composition (g/liter): Bacto beef extract; 3.0, Bacto Peptone; 5.0, Bacto agar; 15.0, Distilled water; 1.0 liter. Pure isolates were maintained on slants of the same medium at 4^{o}C for subsequent identification. Almost all microscopic examinations and biochemical testing used for identification were carried out according to Collins and Lyne and Cheesbrough (1984) [19-20].

Biocides TC/3 Applications and doses:

BIOPOL-TC/3 is an excellent in-can preservative for dispersion paints, dispersion plasters, polymer dispersions, glues, adhesives and sealants. The optimum dose of BIOPOL-TC/3 as preservative should be determined by the means of recommended doses between 0.05 % and 0.25% depending on application.

Adopted techniques:

Weight loss measurements:

Weight loss measurements were carried out by weighing the mild steel specimens before and after immersion in 500 cm^3 acid solutions for different time intervals in the presence and absence of various concentrations of (AE Pom P and Ros).Experiments were also performed at temperature range (298-328K) in HCl solutions. Duplicate experiments were performed in each case and the mean value of the weight loss was determined.

The corrosion rate (C.R.), the inhibition efficiency (IE %) and the surface coverage (θ), that represents the weight of metal surface covered by inhibitor molecules, was calculated using the following equations:

$$I.E.\ \% = [1- (C.R.)_{inh} / (C.R.)_{free}] \times 100 \quad \ldots\ldots\ldots\ldots(1)$$

$$\theta = [1- (C.R.)_{inh} / (C.R.)_{free}] \quad \ldots\ldots\ldots\ldots(2)$$

Open circuit potential measurements (OCP):

The potential of the mild steel electrode (working electrode) was measured against saturated calomel electrode (SCE) (reference electrode) in 1.0 M HCl solution in absence and presence of different concentrations of the used inhibitor.

Potentiodynamic polarization measurements:

The electrochemical cell used in potentiodynamic polarization consists of (three electrodes), working electrode (mild steel), reference electrode (saturated calomel electrode (SCE)) and platinum wire used as counter electrode. The exposed area of working electrode to solution was (1Cm2). For the anodic and cathodic potentiodynamic polarization (Tafel plots) the entire potential scan was programmed to take place within ± 250 mV of the corrosion potential .The measurements were conducted at scanning rate of 0.2 mV/s.

Surface Examinations Techniques:

Scanning Electron Microscope (SEM):

The scanning electron microscope (SEM) is a type of electron microscope giving images of the sample surface by scanning it with a high-energy beam of electrons in a faster scan pattern. SEM images should confirm the electrode surface. The specimens have been rinsed before and after immersion in different solutions.

Energy Dispersive X-ray Analysis (EDAX):

(EDAX) is an analytical technique used for the elemental analysis or chemical characterization of a sample. The

identification of the elements present in the surface of specimens before and after immersion in different solutions will be performed using an energy dispersion X-ray analysis. This technique is used in conjunction with SEM.

Results and discussion:

Gas Chromatography / Mass Spectrometry (GC/MS):

GC/MS give light on the structure of (AE Pom P and Ros) compound (Fig 1 and Table 2) which is obtained from the extraction of AE Pom P and Ros [21].The GC/MS spectrum of (AE Pom P and Ros) exhibits the retention time for (AEPP " Granatonine") 6.33 and 11.78 where for(R "Anthocyanins Derivatives") 65.18 minutes.

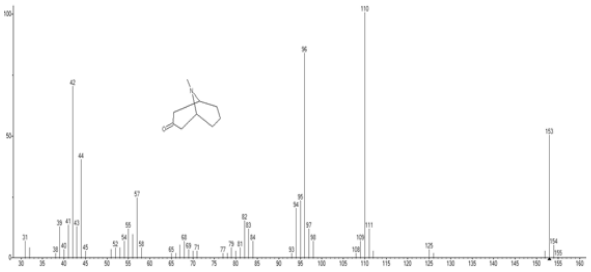

(A) Pomegranate Peel Extract

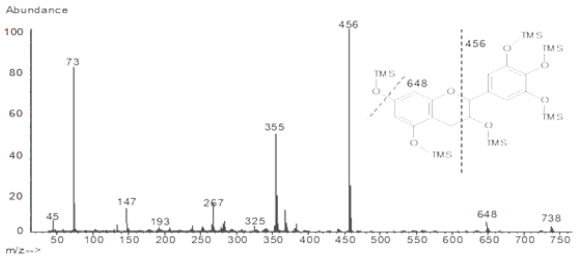

(B) Roselle Extract

Figure 1: GC/MS Scan of (A) Pomegranate Peel Extract and (B) Roselle Extract

Table 2: GC-MS Data Table

	Pomegranate Peel	**Roselle**
Common Name	**Granatonine**	**Anthocyanins Derivatives**
Molecular Formula	$C_9H_{15}NO$	$C_{15}H_{11}O_6^+$
Molecular Weight	153.12	287.24 / 738.31
Retention Time (mins)	6.33 & 11.78	65.18
5 Largest Peaks (m/z)	110, 96, 42, 153 & 44	456, 73, 355, 267 & 147

Evaluation of the stability and antimicrobial activity of AE Pom P and Ros at different temperatures:

The aim of the following experiment is to test the efficiency of TC/3 (anti-bacterial agent) over the natural product extract (AE Pom P and Ros) in different doses (0.05 and 0.25%) and temperature ranges (25 and 60° C).

BIOPOL-TC/3 has shown its effectiveness against the following bacterial microorganisms among others: (Bacillus subtilis, Pseudomonas aeruginosa, Escherichia coli, pseudomonas fluorescens and Staphylococcus aureus).

Fig (2) exhibits in the case of using water as a medium for AE Pom P and Ros, microbial activity presence is a must. Where we tested the AE Pom P and Ros with water in the presence and absence of TC/3 (anti-bacterial agent) at 25 and 60° C. Three vials were prepared, containing 1 gm/100 ml H_2O, the following results were obtained:

1-In the absence of TC/3, microbial contamination appeared on the surface of the extract within 2 - 4 days at 25°C. But in presence of low and high doses of TC/3 no microbial contamination appeared for more than 12 months.

2- Moreover at 60°C, in both cases of low and high doses of TC/3 no microbial contamination appeared.

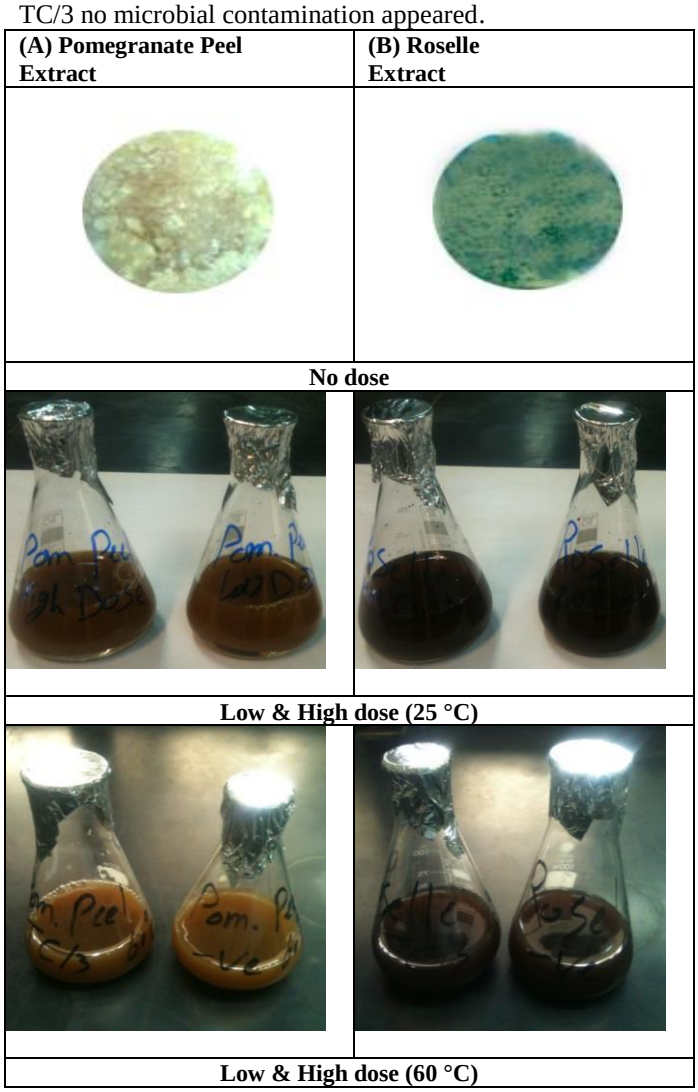

Figure 2: Effect of biocides (BIOPOL-TC/3) on (A) Pomegranate Peel Extract and (B) Roselle Extract by using low and high dose at 25°C and 60°C

Electrochemical Techniques:

Open Circuit Potential (OCP) Measurements:

The way in which a metal changes its potential upon immersion in solution indicates the nature of reaction taking place at its surface. Whilst a shift in potential in the noble direction denotes film repair and healing, a shift in the negative direction significances film destruction and the exposure of more of the surface electrodes to the aggressive solution. The results obtained were used in discussion the mechanism of oxide film growth in aerated test solutions.

The (OCP) for mild steel as a function of time in 1.0 M HCl in absence and in the presence of different concentrations of all under testing aqueous extract of AE Pom P and Ros are studied.

As revealed from inspection of curves (Fig.3) and the results are listed in table (3), the potential of the mild steel electrode is measured directly after immersion as the steady state potential varies with different concentrations of the used (AE Pom P and Ros) solutions (0.01-5.0 g. %). In aqueous extract of AE Pom P and Ros, there is always a general tendency for the OCP to drift with time towards more stable values at which it tends to be stabilized after 30 minutes.

Inspection of OCP curves reveals that. There is always a general tendency for the immersion potential (E_{im}) to shift from negative to the positive direction. The values of steady state potential ($E_{ss.}$) in this case are higher than the value in free acid.

(A) (B)

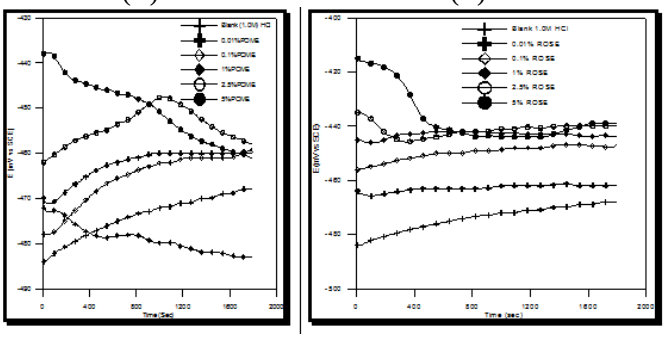

Figure 3: Potential-time curves for mild steel in a)POME, b) ROSE at 1.0M HCl

Table 3: Values of E_{im} and $E_{s.s}$ (mV) for mild steel in 1.0 M HCl at different concentrations of natural product extracts

Media	CONC v/v %	$E_{im.}$(mv)	$E_{s.s}$ (mv)
HCl (blank)	1.0M	-468	-484
ROSE	0.01	-455	-457
	0.1	-450	-445
	1.0	-418	-407
	2.5	-406	-382
	5.0	-440	-417
POME	0.01	-460	-470
	0.1	-460	-478
	1.0	-483	-472
	2.5	-458	-462
	5.0	-461	-438

Potentiodynamic Polarization Measurements:

Fig. (4) represents linear and Tafel polarization curves of l.0M HCl in different concentrations (0.01-5.0 g. %) of (AE Pom P and Ros) at room temperature.

The corrosion kinetic parameters are tabulated in Table (4), showing that the polarization resistance ($R_{p),}$ Tafel slopes constants (β_a, β_c), corrosion potential (E_{corr}), corrosion current density (I_{corr}), corrosion rate (C.R.) and inhibition efficiencies (I.E.%) are function of the of different concentrations of (AE Pom P and Ros).

An inspection of the results presented in Fig. (4) and Table (4) reveals that, increasing the concentration of the additive (AE Pom P and Ros).shows the following:

1. It is clearly that different concentrations of (AE Pom P and Ros) shifted both anodic and cathodic branches of polarization curves to lower values of current density indicating that all concentration act as mixed type inhibitors. The addition of different concentrations of (AE Pom P and Ros) to HCl solution reduces the anodic dissolution of mild steel and also retards the cathodic hydrogen evolution reaction.
2. The corrosion potential (E_{corr}) shifted slightly to more positive values while the corrosion current (I_{corr}) decreases with increasing the inhibitor concentration, indicating the inhibiting effect of these compounds.
3. The variable values of the cathodic Tafel slopes suggest that the inhibition action of (AE Pom P and Ros) such compounds occurs by simple blocking of the electrode surface area [22].
4. The obtained results indicated that (AE Pom P and Ros) compounds inhibit HCl corrosion of mild steel via their adsorption on both anodic and cathodic active sites without modifying the mechanism of corrosion reaction. This means that the adsorbed inhibitor molecules block the surface active sites and decrease the area available for hydrogen evolution and metal dissolution reactions [23].
5. The (I.E.%) calculated was found to increase with increasing the (AE Pom P and Ros).concentration.

a) Linear polarization **b) Tafel polarization**

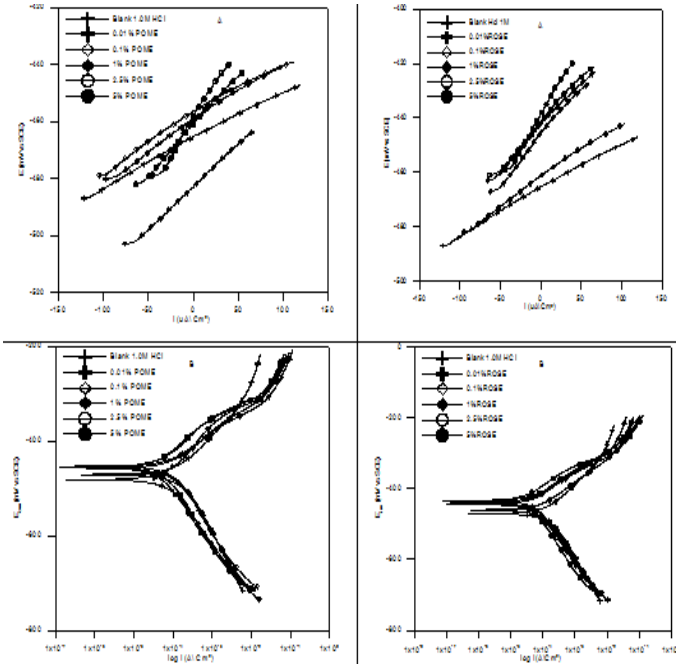

Figure 4: Linear and Tafel plots polarization curves of mild steel in different concentrations of (A) POME, (B) ROSE at 1.0M HCl

a) Linear polarization **b) Tafel polarization**

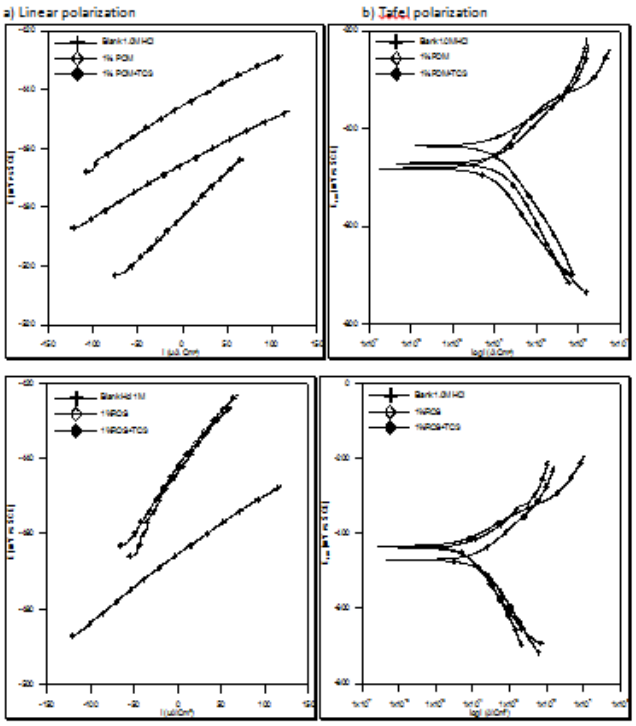

Figure 5: Linear (a) and Tafel plots polarization (b) curves of mild steel in 1.0M HCl at different natural product extracts with and without biocide (TC/3)

Table 4: Polarization parameters for mild steel in 1.0 M HCl at different concentrations of natural products extracts

Test Solution	Conc v/v%	R_p Ω	Tafel Slopes βa (mV/decade)	Tafel Slopes βc (mV/decade)	Ecorr (mV)	Icorr µA/Cm^2	C.R (mpy)	I.E (%)	Surface coverage θ
HCl 1.0M	-	180	124.5	187.6	471	225.3	207.73	-	-
ROSE	0.01%	208	72.27	130.3	461	90.27	83.23	60	0.60
	0.1%	312	81	136.7	444.9	62.6	57.72	72	0.72
	1%	319	55.93	130.1	434.1	48.04	44.29	79	0.79
	2.5%	346.8	63.48	117.1	440.4	41.6	38.36	82	0.82
	5%	517	54.79	113.2	435.9	20.38	18.79	91	0.91
POME	0.01%	185.3	69.78	131.7	458.1	91.48	84.35	59	0.59
	0.1%	192.6	59.72	123.8	453.6	76.78	70.79	66	0.66
	1%	299	79.91	105.6	481.5	52.38	48.30	77	0.77
	2.5%	344	73.4	116.1	456.4	36.6	33.75	84	0.84
	5%	354.4	63.68	102.9	454.7	32.83	30.27	85	0.85

Table 5: Polarization parameters for mild steel in 1.0M HCl at natural product extracts with and without biocide

Test Solution	R_p Ω	Tafel Slopes βa (mV/decade)	Tafel Slopes βc (mV/decade)	Ecorr (mV)	Icorr µA/Cm^2	C.R (mpy)	I.E (%)
HCl 1.0M	160	124.5	187.6	471	225.3	207.73	-
ROS	500	55.93	130.1	434.1	40	36.88	82
ROS+TC/3	427	80.7	185.4	439	84	77.45	63
POM	299	79.91	105.6	481.5	52.38	48.30	77
POM+TC/3	177	72.23	138.9	435.7	121	111.57	46

Evaluation of (AE Pom P and Ros) compounds and biocide on the corrosion rate in HCl:

Linear and Tafel polarization measurements were performed on mild steel in 1.0M HCl with and without AE Pom P and Ros inhibitors (1.0% w/v) and optimum dose biocide (0.1% v/v) are given in Fig (6) and the corrosion parameters are given in Table (4).This clearly indicates that, although the optimum dose of biocide which give good stability of (AE Pom P and Ros) as eco-friendly corrosion inhibitor (or may be any other natural products) for more than one year ,it decrease the inhibition efficiency about 20% due to its slightly acidic in nature (pH=4), therefore we will try in future to study effect of pH of biocide on the stability of natural products.

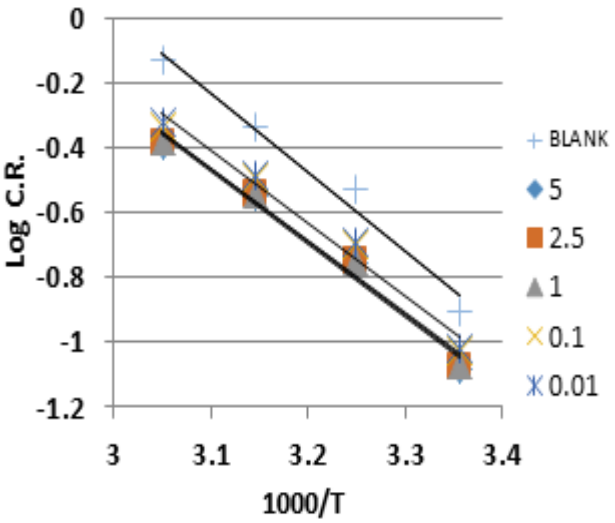

(A) Pomegranate Peel

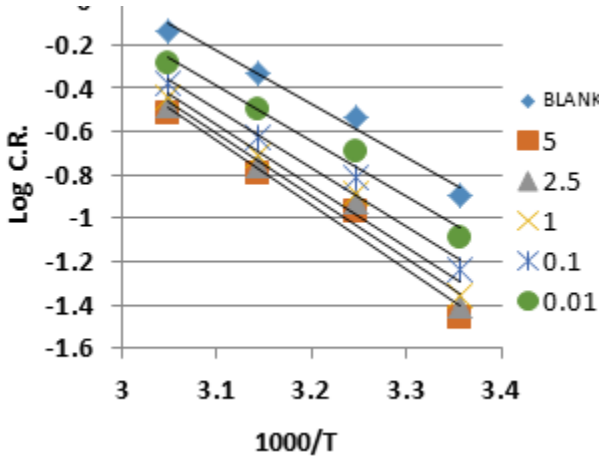

(B) Roselle

Figure 6: Arrhenius plots for mild steel in 1.0 M HCl in the absence and presence of different concentrations of (A) Pom. Peel & (B) Ros.

Weight Loss Measurements:

Weight loss measurements were carried out for mild steel in 1.0M HCl in the absence and presence of different concentrations of AE Pom P and Ros. It is noted that the IE% increases steadily with increasing the concentration of AE Pom P and Ros and decrease with rising the temperature from 298-328 K. The inhibition efficiency (IE %) and surface coverage (Θ) were calculated by equations (1, 2).

Thermodynamic and Adsorption Considerations:

To investigate the mechanism of inhibition and to determine the activation energy of the corrosion process, weight loss of mild steel in 1.0 M HCl was determined at various temperatures (298-328 K) in the absence and presence of different concentrations of (AE Pom P and Ros).

In an acidic solution the corrosion rate is related to temperature by the Arrhenius-type equation [24]:

$\log C.R. = [-Ea / 2.303\ RT] + \log A$ …..…… (3)

Where (C.R.) is the corrosion rate, Ea is the apparent activation energy, R is the molar gas constant, T is the absolute temperature and A is the frequency factor. Fig. (6) shows the plot of log C.R. versus 1/T. Linear plots were obtained for different AEG compounds. The values of Ea were computed from the slope of the straight lines and are listed in Table (6). It is clear from this table that Ea values in presence of the AEG are higher than in their absence in case of Ros. But lower in Pom. P. Inspection of these data reveals that the apparent activation energy Ea in HCl in the absence of (AE Pom P and Ros) was 46.886 k j/mol$^{-1.}$.

Low activation energy means fast reaction and high activation energy means slow reaction. High activation energy corresponds to a reaction rate that is very sensitive to temperature. Conversely small activation energy indicates a reaction rate that varies only slightly with a temperature. If reaction has zero activation energy, its rate is independent of temperature. In some cases , activation energy (E_a) is found negative which indicates that the rate decreases when temperature is raised and such behaviour is a signal that reaction has a complex mechanism[25,26].

Enthalpy and entropy of activation ΔH*and ΔS* were obtained by applying the transition state equation:

$$C.R. = [RT/Nh] \exp(\Delta S^*/R) \exp(-\Delta H^*/RT) \quad \ldots\ldots (4)$$

$$\log C.R. = \log[RT/Nh] + (\Delta S^*/R) - (\Delta H^*/RT) \quad \ldots\ldots (5)$$

Where h is the Plank's constant, N is the Avogadro's number, T is the absolute temperature and R is the universal gas constant. Plots log[C.R./T] as a function of 1/T were shown in Fig. (7). Straight lines were obtained with a slope of (-ΔH*/ RT) and an intercept of log[R/Nh] + (ΔS*/ R), being the values of ΔH*and ΔS* calculated, and listed in Table (6). While an endothermic adsorption process (ΔH* > 0) is attributed unequivocally to chemisorption, an exothermic adsorption process (ΔH* < 0) may involve either physisorption or chemisorption or a mixture of both processes [50]. In the present work, the positive sign of the activation enthalpy (ΔH*) reflects the endothermic nature of the steel dissolution process and that the dissolution of steel is difficult. The order of the phenomena ascribed by the negative values of (ΔS*), may probably be explained by the possibility of the formation of iron complex on the metal surface [27].

In order to get a better understanding of the adsorption mode of the inhibitor on the metal surface, the data were tested graphically by fitting them to various isotherms to find the best isotherm which describes this study. The value of correlation coefficient (R^2) was used to determine the best fit isotherm. Langmuir adsorption isotherm was found to fit well the experimental data. According to this isotherm, θ is related to the C and adsorption equilibrium constant $K_{ads.}$, via the following equation [28].

$$C/\theta = [1/K_{ads.}] + C \quad \ldots\ldots (6)$$

Using equation (6), plots of log (C/θ) versus C gave straight lines Fig. (8), with a slope of around unity confirming that the adsorption of different AEG on mild steel surface in hydrochloric acid solution obeys the Langmuir adsorption isotherm at 25^{o}C (similar data are obtained at different temperatures). The values of Langmuir adsorption parameters obtained from the plots are recorded in Table (7).

The results show that the slopes and R^2 values are very close to unity indicating strong adherence of the adsorbed inhibitors to the assumptions of Langmuir [29].

The equilibrium constant of adsorption obtained from the slopes of Langmuir isotherms was used to calculate the free energy for the adsorption of different (AE Pom P and Ros) on the surface of mild steel. The free energy of adsorption of different (AE Pom P and Ros)on the metal surface is related to the equilibrium constant of adsorption according to equation (7)

$$K_{ads.} = [1/55.5] \exp(-\Delta G_{ads.}/RT) \quad \ldots\ldots (7)$$

Where R is the universal gas constant , $\Delta G_{ads.}$ is the free energy of adsorption and 55.5 is the concentration of water in solution (mol L^{-1}) [30].

The enthalpy and entropy of adsorption ($\Delta H_{ads.}$ And $\Delta S_{ads.}$) can be calculated using equation (8).

$$\ln K_{ads.} = [\ln 1/55.5] - (\Delta H_{ads.}/RT) + (\Delta S_{ads.}/R) \quad \ldots\ldots (8)$$

Using equation (9), the values of $\Delta H_{ads.}$ and $\Delta S_{ads.}$ were evaluated from the slope and intercept of plot ln $K_{ads.}$ versus 1 / T, Fig. (9).The values of $\Delta G_{ads.}$, $\Delta H_{ads.}$ and $\Delta S_{ads.}$ are listed in Table (7). From the results, it is significant to note that the calculated values of $\Delta G_{ads.}$ are negative indicating that the adsorption is a spontaneous process. Generally, the values of $\Delta G_{ads.}$ around -20 KJ mol^{-1} or lower are consistent with the electrostatic interaction between charged molecules and the charged metal surface (physisorption), while those around -40 KJ mol^{-1} or more negative involve chemisorption [31]. In the present study, the values of $\Delta G_{ads.}$ranged from (-31.67 to -36.99 and -29.26 to 27.27 for AE Pom P. and Ros. respectively) at temperatures ranged from (25 to 55 °C), which probably means that both physisorption and chemisorption are taking place.

The values of $\Delta S_{ads.}$ are positive in the adsorption process and this could be explained as follows:

The thermodynamic values which are obtained the algebraic sum of the adsorption of organic molecules and desorption of water molecules [32], therefore, the gain in enthalpy is attributed to the increase in solvent entropy [32, 33]. The values of $\Delta H_{ads.}$ provides further information about the mechanism of corrosion inhibition. The endothermic adsorption process is ascribed unambiguously to chemisorption and an exothermic process may involve either physisorption or chemisorption or a combination of both [34]. In the present study, the negative values of $\Delta H_{ads.}$ obtained indicate a combination of both physisorption and chemisorption processes. Moreover the $\Delta H_{ads.}$values are exothermic and endothermic process for Ros. and Pom.P. respectively.

The values of$\Delta H_{ads.}$ and$\Delta S_{ads.}$ can also be calculated by using the following equation [35]:

$$\Delta G_{ads.} = \Delta H_{ads.} - T\,\Delta S_{ads.} \quad \ldots\ldots (9)$$

Using equation (9), the plot of $\Delta G_{ads.}$ versus T gives a straight line (Fig. (10)) with a slope of $-\Delta S_{ads.}$ and intercept of $\Delta H_{ads.}$ The values obtained are well correlated with those obtained from equation (8).

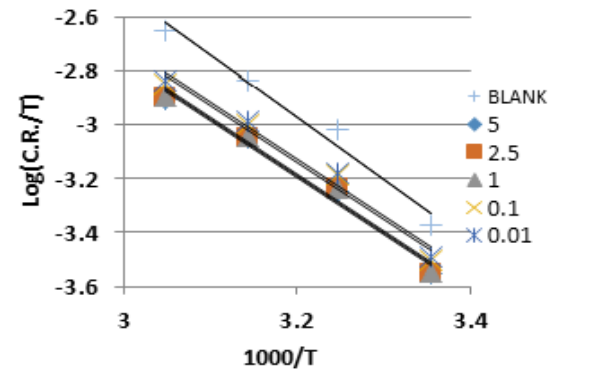

(A) Pomegranate Peel

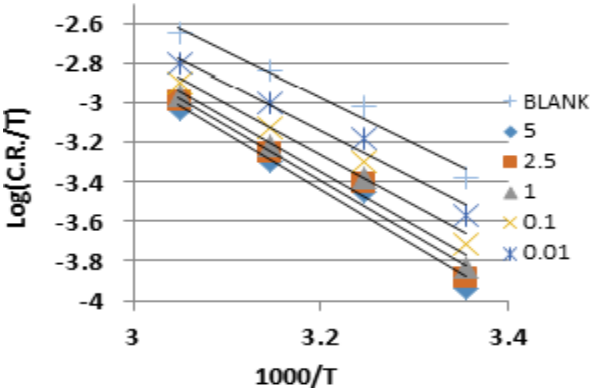

(B)Roselle

Figure 7: Alternative Arrhenius plots for mild steel dissolution in 1.0 M HCl in the absence and presence of different concentrations of (A) Pom. Peel & (B) Ros

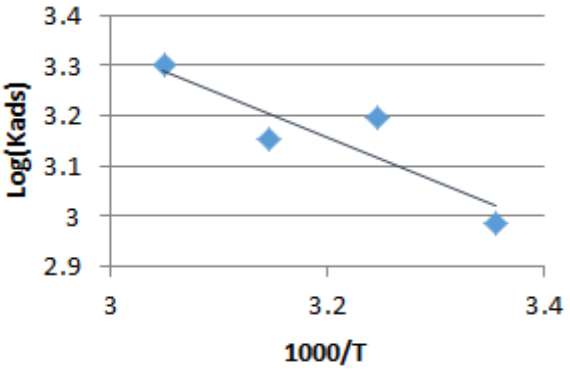

(A) Pomegranate Peel

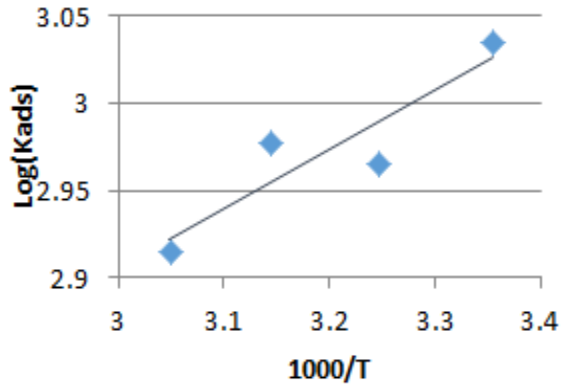

(B)Roselle

Figure 9:Van't Hoff equation for (A) Pom. Peel & (B) Ros

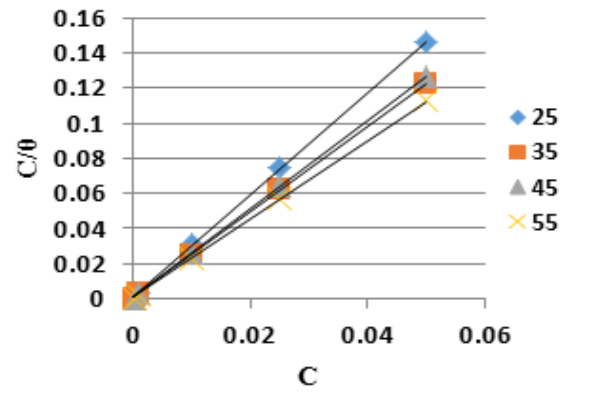

(A) Pomegranate Peel

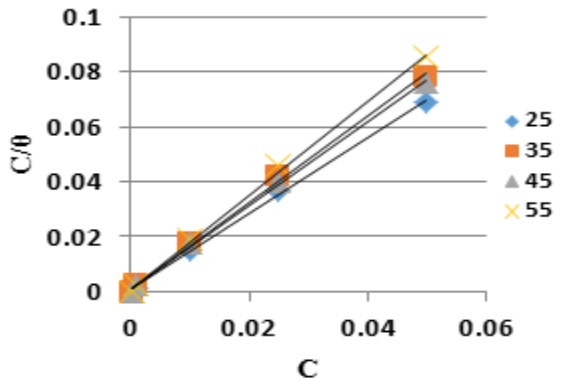

(B)Roselle

Figure 8: Langmuir adsorption isotherm for (A) Pom. Peel & (B) Ros. on mild steel in 1.0 M HCl at different temperatures

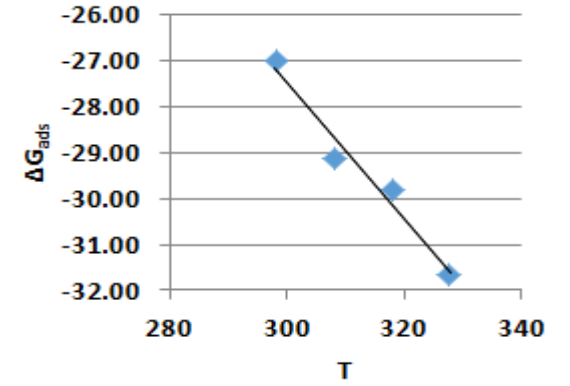

(A) Pomegranate Peel

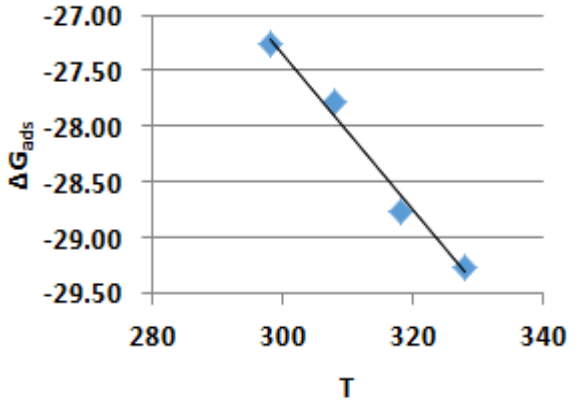

(B)Roselle

Figure 10: plot of ΔG_{ads} versus absolute temperature for (A) Pom. Peel & (B) Ros

Table 6: Activation parameters for mild steel in 1.0 M HCl in the absence and presence of different concentrations of Pom. & Ros

Dye	Conc. (w/v) %	Ea	ΔH*	ΔS*
BLANK	0	46.88	44.28	-112.75
Pom. Peel	5	42.90	40.30	-129.74
	2.5	42.91	40.31	-129.60
	1	42.92	40.32	-129.45
	0.1	42.90	40.31	-128.66
	0.01	43.07	40.48	-127.89
Roselle	5	56.67	54.07	-90.32
	2.5	55.37	52.77	-93.60
	1	54.32	51.72	-96.18
	0.1	51.55	48.95	-103.39
	0.01	48.82	46.22	-109.84

Table 7: Thermodynamic parameters for adsorption of Pom. & Ros. in 1.0 M HCl at different temperatures from Langmuir adsorption isotherm

Natural Product	Temperature, K	R^2	K_{ads}, L mol^{-1}	ΔG_{ads}, kJ mol^{-1}	ΔH_{ads}, kJ mol^{-1}	ΔS_{ads}, J $mol^{-1}K^{-1}$	
Pom. Peel	298	0.997	966.44	-26.99	16.87	147.44	a
	308	0.997	1571.15	-29.14			
	318	0.997	1420.63	-29.82	16.87	103.06	b
	328	0.996	1991.19	-31.67			
Roselle	298	0.997	1082.69	-27.27	-6.4707	69.65	a
	308	0.997	922.45	-27.77			
	318	0.997	949.47	-28.75	-6.46	103.06	b
	328	0.998	822.61	-29.26			

(a) values obtained from Eq. (5) (b) values obtained from Eq. (6)

Table 8: Chemical composition of mild steel by using EDAX spectra

specimen	Fe %		O %		Cl %		Si %		Al %		N %	
	Element %	Atomic %	Element %	Atomic %	Element %	Atomic %	Element %	Atomic %	Element %	Atomic %	Element %	Atomic %
Pure mild steel	99.25	95.82	0.75	4.28	---	---	---	---	---	---	---	---
Mild steel in (1.0 M HCl)	94.01	82.33	5.51	16.83	---	---	0.48	0.84	---	---	---	---
Mild steel in (1.0 M HCl + Ros.)	92.173	77.443	7.700	22.363	0.087	0.113	---	---	0.047	0.083	---	---
Mild steel in (1.0 M HCl + Pom.)	28.007	9.527	42.057	49.913	0.030	0.013	---	---	---	---	29.907	40.547

Surface Morphology of the Metal Electrodes:

The scanning electron microscope images and energy dispersive X-ray analysis further supported the formation of a surface film by the inhibitors and their interaction with surface atoms of mild steel.

Scanning Electron Microscope (SEM) Analysis:

Fig (11 A) illustrates the morphology of the surface of polished mild steel electrode before exposure to corrosion media (blank).

The specimens were subjected to microscopic examination at x 1500. The micrograph shows a characteristic inclusion, which was probably an oxide inclusion. Fig (11 B) shows SEM image of the surface of the studied mild steel specimen after immersion in 1.0 M HCl solution for 24 hr. The micro graph reveals that, the surface was strongly damaged. The corroded areas are shown as black grooves in the specimen with gray and white zones, which correspond to the dandruff of iron oxide. It suggested an uncovered surface of metal electrode severally corroded. The highly oxidized phase perhaps formed in air when desiccated under no protection for the surface.

Fig (11 C and D) show SEM images for the surface of another mild steel specimen after immersion for the same time interval in 1.0 M HCl solution containing 1.0 x 10^{-3}(AE Pom P and Ros) extract. The micrograph reveals that, the inhibited metal surface is smoother than the uninhibited surface, a good protective film present on the metal surface. This confirms the highest inhibition efficiency of the inhibitors.

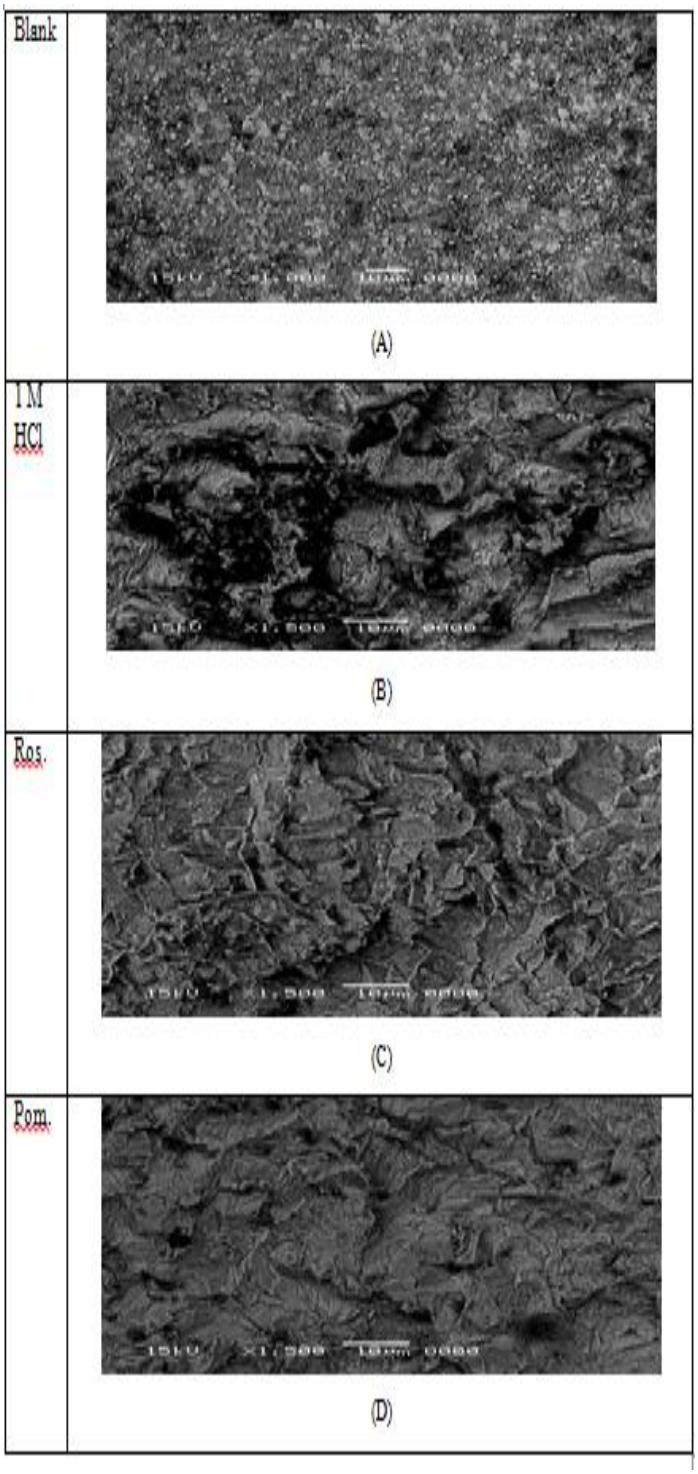

Figure 11:
(A) SEM image of polished mild steel surface
(B) SEM image of mild steel exposed to 1.0 M HCl.
(C) Mild steel exposed to 1.0 M HCl / 1.0 % W/V from Ros
(D) Mild steel exposed to 1.0 M HCl / 1.0 % W/V from Pom

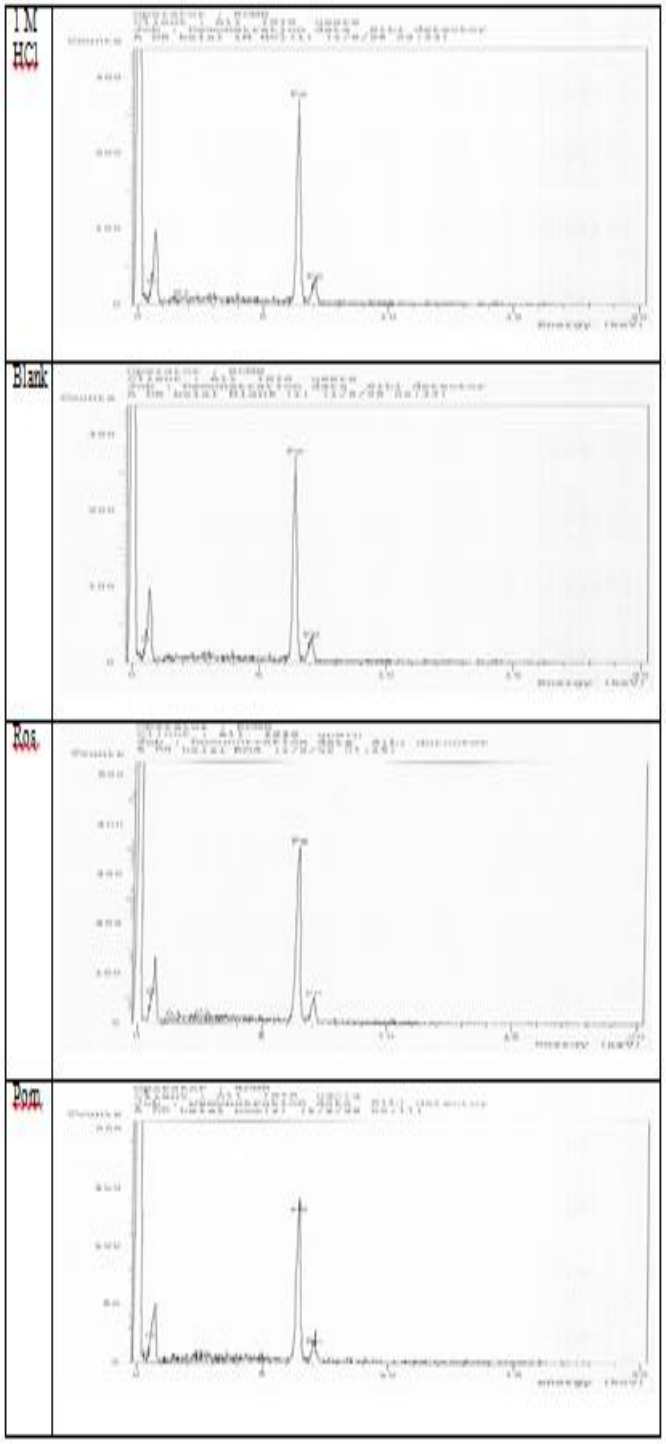

Figure 12: EDAX examination of the area of mild steel which represent (A) Blank (B) immersed in 1.0M HCl for 24 hr. (C) and (D) immersed in 1.0 M HCl in present of AE Pom P and Ros for 24 hr

Energy Dispersive X-ray Analysis (EDAX):

It is important to take into consideration the percentage of the elements present on the surface of the mild steel. The EDAX analysis of the surface reveals the presence of oxygen and iron, suggesting therefore the presence of iron oxide / hydroxide (Fig (12)). The presence of the peaks of carbon, nitrogen, chloride, silicon and sulpher is explained by the adsorption of the inhibitor (AE Pom P and Ros) on the products of corrosion of the mild steel.

Conclusion:

From the overall experimental results the following conclusion can be deduced:

1-In the absence biocide, microbial contamination appeared on the surface of the extract within 2 - 4 days at 25^{o}C. But in presence of low and high doses of TC/3 no microbial contamination appeared for 12 months.

2-The AE Pom P and Ros shows good performance as corrosion inhibitor in 1.0 M HCl.

3- Although the optimum dose of biocide which give good stability for both (AE Pom P and Ros) as corrosion inhibitor

for more than one year ,it decrease the inhibition efficiency about 20% due to its slightly acidic in nature (pH=4).

4-The inhibition efficiency increases with increase in the concentration of (AE Pom P and Ros), but decreases with an increase in temperature.

5- The (AE Pom P and Ros) influence both the cathodic and anodic reactions in the HCl solution. This indicates that the additive act as mixed- type inhibitors.

6- The (AE Pom P and Ros) inhibits the corrosion by getting adsorbed on the metal surface following Langmuir adsorption isotherm.

References

1-B. Bavarian, L. Reiner, "Corrosion,Protection of Steel Rebar in Concrete with Optimal Application of Migrating Corrosion Inhibitors", MCI 2022, 2–3, (2003).

2- A. Singh, E.E. Ebenso, and M.A. Quraishi, International Journal of Corrosion Volume 2012 (2012), Article ID 897430, 20 pages.

3- B.E.A. Rani and B.B.J. Basu, International Journal of Corrosion, 2012 (2012) 1-15.

4- S. Nuryanti, S. Matsjeh, C. Anwar, T.J. Raharjo and B. Hamzah, European Journal of Chemistry 4 (1) (2013) 20-24.

5- Amor, B.; Allaf, K. J. Food Chem. 2009, 115, 820-825.

6- Ologundudu, A.; Ologundudu, A. O.; Ololade, I. A.; Obi, F. O. Afr. J.Biochem. Res. 2009, 3(4), 140-144.

7- Harborne, J. B. Phytochemical Methods. A Guide to Modern Techniques of Plant Analysis, 2nd edition, Chapman & Hall, 1984.

8- Torskangerpoll; Andersen, Q. M. J. Food Chem. 2004, 89, 427-444.

9- P. Mena, L. Calani, C. Dall'Asta , G. Galaverna , C.G Viguera , R. Bruni , A. Crozier and D. Del Rio, Molecules 17 (2012) 14821-14840.

10- H. Goodarzian, and E. Ekrami, World Applied Science Journal, 8 (2010) (11): 1387-1389.

11- S. Adeel, , S. Ali, , I. Bhatti, and F. Zsila,. Asian J. Chem,. 21 (5) (2009) 3493- 3499.

12- H. Tiwari, P. Singh, P. Mishra and P. Shrivastava. IJFTR, 35 (2010) 272-276.

13- S.S. Kulkarni, A.V. Gokhale, U.M. Bodake, G.R. Pathade, Universal Journal of Environmental Research and Technology, 1 (2) (2011) 135-139.

14- K.L. Nyam, M.M. Wong, K. Long, and C.P. Tan, International Food Research Journal 20 (2) (2013) 695-701.

15- Baklola, E. A. The impact of sanitary and food industrial wastes on water quality of Menyat Samanoud agriculture drain at El–Dakahliya Governorate., Egypt, Fac. Sci., Tanta., Univ., M. Sc. Thesis. (2013).

16- American Public Health Association "APHA". Standard Methods for the Examination of Water and Wastewater (21st ed.), Washington, D. C. (2005)

17- Pettibone, G. W. The use of lauryal treptose broth containing 4-methyl umbelliferyl- beta- D-glucuronide "MUG" to enumerate *E.coli* form fresh water sediment. Lett. Appl. Microbiol. 15(5)(1992) 190-192.

18- Cappuccino, J. G. and Sherman, N. Microbiology: A laboratory manual. 6th ed. Benjamin Cummings, San Francisco.(2002)

19-Collins, C.H. and Lyne, P.M. Microbiological methods. 5th Ed. 450, Butterworth, England.(1984)

20 -Cheesbrough, M. "Microscopical examination of specimens" and "Biochemical testing of microorganisms", in: Medical laboratory manual for tropical countries. Tropical health technology, Butterworth-Heinemann Ltd. Printed in Great Britain at University press, Cambridge, 2(1984).26-39 and 58-69.

21- K.ASHOK KUMAR1 AND K.VIJAYALAKSHMI, International Journal of Pharma and Bio Sciences , 2(4) (2011) B-461-468.

22-M. Vracar Lj and D.M. Dragic. Corros. Sci. 44 (2002) 1669.

23-B. El-Mahdi, B. Mernari, M. Traisnel, F. Bentiss and M. Lagrenee. Mater. Chem. Phys. 77 (2002) 489.

24-E.E. Ebenso, H. Alemu, S.A. Umoren and I.B. Olet. Int. J. Electrochem. Sci. 3 (2008) 1325-1339.

25-E.E. Ebenso, H. Alemu, S.A. Umoren and I.B. Obot. Int. J. Electrochem. Sci. 3 (2008) 1325-1339.

26-S.A. Umoren and E.E. Ebenso. Pigment and Resin Technol. 37 (8) (2008) 173.

27-M.Y. Mourad, S.A. Seliman and S.M. Abd El-Metaal. Bull. Soc. Chim. Fr. 128 (1991) 832- 836.

28-I. Langmuir, J. Am. Chem. Soc. 39 (1947) 1848-1850.

29-S.A. Ali, M.T. Saeed and S.U. Rahman. Corros. Sci. 45 (2005) 253.

30-E. Khamis. Corrosion. 46 (1990) 476-484.

31-E. Bensajjay, S. Alehyen, M. El-Achouri and S. Kertit. Anti-Corros. Meth. Mater. 50 (2003) 402.

32-E.T. Kumar, S. Viswanatham and G. Udayabhanu. Corros. Eng. Sci. Technol. 39 (2004) 327.

33-B. Ateya, B. El-Anadouli and F. El-Nizamy. Corros. Sci. 24 (1984) 509.

34-S.A. Ali, A.M. El-Shareef, R.F. Al-Ghamdi and M.T. Saeed. Corros. Sci. 47 (2005) 2659.

35-S.S. ShivaKumar and N.K. Mohana. Int. J. Electrochem. Sci. 7